Bulgarian Chemical Communications, Volume 55, Special Issue A (pp. 12-18) 2023 DOI: 10.34049/bcc.55.A.0002

Spectroscopic studies on the interaction of BSA and anisaldehyde

A. Singh[1,2*], D. K. Sinha[3], K. K. Thakur[2]

[1]*M. J. P. Rohilkhand University, Bareilly, UP, India*
[2]*Chandigarh University, Gharuan Punjab, 140301, India*
[3] *K G K College, Moradabad, UP, India*

Received: March 23, 2023; Revised: April 23, 2023

The flavouring molecule anisaldehyde (AA) is present in anise and is regarded as one of the most important flavouring chemicals in the world. Numerous yeast and mould strains have been found to be resistant to p-anisaldehyde. In this research paper, we investigated the bovine serum albumin (BSA) binding profile using both experimental and computational techniques, because the interaction with serum albumins may be essential in determining their pharmacological characteristics. The structural alteration of the BSA upon the addition of AA was investigated, as well as the binding parameters and method of binding. Results from UV-vis spectroscopy and fluorescence quenching studies suggested that AA and BSA can form a ground state complex. Meanwhile, thermodynamic characteristics (negative ΔH^0 and ΔS^0 values) showed that the formation of the AA-BSA complex is primarily influenced by hydrophobic interactions and hydrogen bond forces. AA appreciably alters the 2° structure of BSA, according to circular dichroism synchronised fluorescence spectra.

Keywords: Anisaldehyde, BSA, Interaction, Fluorescence, UV

INTRODUCTION

Due to the wide range of medicinal applications and absence of undesirable side effects, natural chemicals and their derivatives are the potential molecules for drug discovery. These natural compounds offer a wide range of therapeutic benefits because of their distinct chemical and structural composition [1, 2]. Many organic compounds have antioxidant and anti-cancer properties and are exploited in the creation of novel medications [3, 4]. Polyphenols, which are present in many different foods and beverages, including tea, coffee, nuts, vegetables, and fruits, are substances that occur naturally and are primarily being studied [5-7].

Anisaldehyde (AA), is a naturally occurring phenolic compound and one of the most common flavouring substances in the world [8]. It is a perennial herb with a long history of cultivation in South Asia, particularly India, and the Mediterranean region. The compound is present in several plant species like anise, cumin, fennel and garlic. Anisaldehyde, also known as anisic aldehyde, is an organic molecule composed of a benzene ring that has a methoxy and aldehyde group substituted on it. According to earlier research, p-anisaldehyde has antifungal properties that make it effective against a variety of yeast and mould strains in lab media, fruit purees, and fruit juices [9, 10]. Additionally, it has been claimed that anise fruit extracts provide therapeutic benefits for a number of ailments, including gynaecological and neurological diseases. Especially in paediatrics, the oil is used as a carminative and expectorant, in syrups, flavouring and spice. It is also used as a raw material for the synthesis of drugs such as amoxicillin.

The bio-distribution of endogenous and exogenous substances is predominantly carried out by serum albumins, which are the utmost prevalent proteins in blood plasma [11]. Drug-protein binding studies are important for figuring out a drug's biological effects because they can offer important details about a drug's pharmacological and pharmacodynamic therapeutic effects. Knowing the precise position of the drug binding site on a protein can help us better recognize how a drug is distributed throughout the body and how it interacts with other medications [12]. Bovine serum albumin (BSA), is a well-known protein with 76% similarity to human serum albumin (HSA). The binding capability of anisaldehyde with skin proteins is therefore investigated using BSA as a model protein. Two drug-binding sites, subdomain IIA (Sudlow I) and subdomain IIIA, are found in hydrophobic pockets in the BSA's single-chain globular protein structure, which comprises 583 amino acids (Sudlow II). There are two tryptophan residues nearby subdomains IA and IIA, Trp 134 in and Trp212. Utilizing multiple spectroscopic methods including UV-Vis absorption, steady-state fluorescence, synchronous

* To whom all correspondence should be sent:
E-mail: anju.chemistry@cumail.in

fluorescence, FTIR, and circular dichroism (CD), the current research examines the structural and thermodynamic characteristics of anisaldehyde binding to BSA. Through the use of molecular docking, the binding interactions within the binding pockets were demonstrated.

EXPERIMENTAL

Starting materials

Bovine serum albumin (BSA) devoid of essential fatty acids was purchased from Sigma-Aldrich Bangalore, India. Anisic aldehyde was received as a gift by Nishant Aromas, Mumbai (Maharashtra). We bought warfarin and ibuprofen from Tokyo Chemical Industry (TCI) Co., Ltd. The other reagents and chemicals utilized in the study were of analytical grade and didn't need any extra purification. Doubly distilled water was utilised during the studies.

Spectrophotometric titration

On a UV-1900iUV spectrophotometer (Shimadzu, Japan) with an 1-cm quartz cell, absorption spectra of AA binding to BSA were captured while scanning from 200 to 800 nm. UV-Vis titrations were conducted by gradually adding anisaldehyde (0-32 μM) to BSA (10 μM) in a phosphate buffer solution of pH 7.4. The solvent absorption was deducted from the spectra of BSA and BSA-AA complex absorptions in order to remove interference.

Measurements of fluorescence quenching by titration

Fluorescence spectra were captured using an RF-6000 spectrofluorometer, Shimadzu Scientific Instruments, Japan at excitation wavelength of 295 nm and an emission wavelength of 300–450 nm @ 240 nm/min, while keeping the excitation and emission slit width at 5.0 nm. In titration studies, AA concentrations ranged from 0.25 μM to 4.5 μM at three distinct temperatures of 303 K, 308 K, and 313 K that were regulated *via* a water bath. For the site marker assays, the AA and BSA interaction was conducted with equimolar concentrations of the site markers.

Measurements based on circular dichroism

In order to validate the outcomes of spectra, CD was applied. The BSA and anisaldehyde were mixed in molar ratios of 1:0, 1:1, and 1:5. After every addition, the solution was thoroughly shaken, and incubated for 2.0 min at ambient temperature, and its CD was detected in the 200–300 nm range at 1.0 nm band width. A minimum of three scans @ 50.0 nm/min were used to average the spectra. Baseline corrections were made to all CD spectra using blank solutions.

Docking of molecules

The Lamarckian genetic algorithm was considered to execute the molecular docking using Autodock 4.2 [16–18]. From the Brookhaven Protein Data Bank and PubChem, respectively, we were able to retrieve the structures of BSA and AA. The complete protein was chosen for docking with all polar hydrogen atoms. BSA was given responsibility for the Kollman allegations in part. The protein was configured to be stiff, and docking does not take solvent molecules into account. The minimal binding free energy conformation of the MC-AA complex was displayed using molecular graphics, as well as analyses performed with UCSF Chimera and Ligplot+ v2.2.

RESULTS AND DISCUSSION

Absorption measurements by UV-vis spectrometry

It is an effective method to explore the development of protein-drug complexes [13, 14]. The microenvironment around the chromophores has an impact on the protein spectrum [15]. Figures depict how AA has an impact on the spectra of BSA. A discernible strong absorption peak can be seen at 277 nm, as revealed in Fig.1(a). The figure displays that peak intensity increases with slight red shifting as AA concentrations rise, supporting the interaction between AA and BSA.

Fluorescence quenching of BSA induced by anisaldehyde

The fluorescence quenching approach has been extensively used to explore the binding constant, the number of binding sites, and thermodynamic factors [16, 17]. In essence, variations in the intensity of protein fluorescence are picked up at the wavelength of maximal emission. TheAA-BSA complex, as depicted in Fig.1(b), is created when AA is added to the BSA solution. With rising AA concentrations, BSA fluorescence emission is quenched. Figure 1 demonstrates that the Trp residue [18] is primarily responsible for the fluorescence peak in BSA at about 335.0 nm. Regular quenching of BSA fluorescence was seen with the addition of anisaldehyde on a continuous basis. On additions of anisaldehyde (0.0625×10^{-3} M) to BSA (10×10^{-6} M) quenched the fluorescence at 335 nm by 70% at a molar ratio of 0.45 ([anisaldehyde]/[BSA]). The red shift of the fluorescence maxima from 335 nm to 340 nm was related to the quenching of BSA's fluorescence. These results showed that BSA and AA clearly interacted.

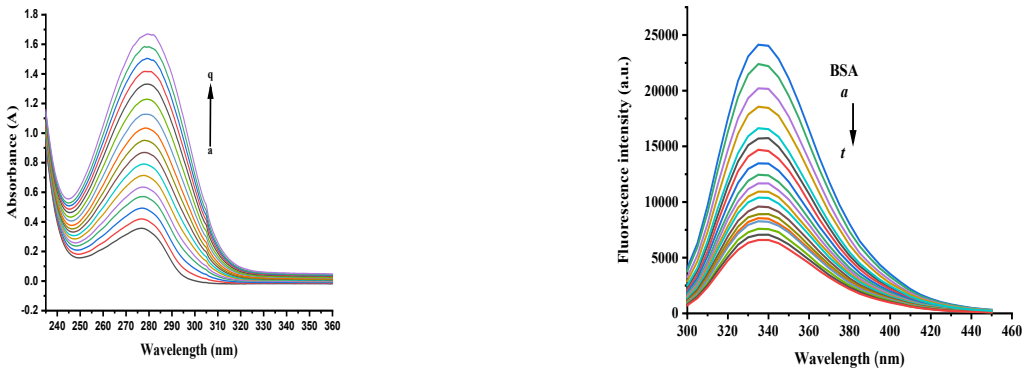

Figure 1. (a) UV-visible spectra at 298 K and pH 7.4 of BSA (C_{BSA} = 10µM)) and AA (C_{AA} = (0-32 µM); (b) Fluorescence quenching of BSA

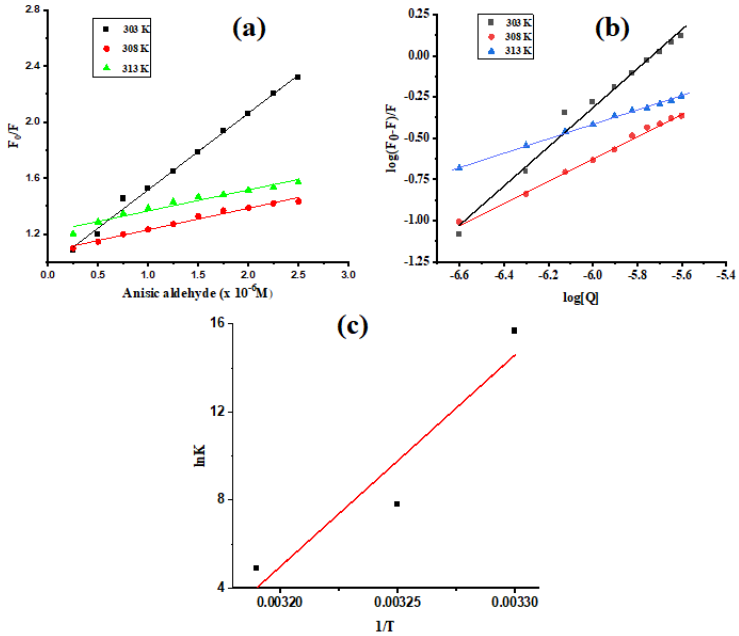

Figure 2. (a) Stern-Volmer graphs for the BSA-AA system at several temperatures; (b) Graph of log (Fo-F)/F *vs* log[Q] at three different temperatures; (c) Plot for Van't Hoff equation

The Stern-Volmer equation might be used to define the concentration-dependent FI quenching under these circumstances [16, 19, 20]. The binding properties at numerous temperatures were investigated according to the following relation:

$$\frac{F_0}{F} = 1 + K_{sv}[Q] \quad (1)$$

Fluorescence levels of BSA before and after bonding with AA expressed as F_o and F respectively. [Q] is the concentration of the quencher, and K_{SV} is the Stern-Volmer constant. The K_{SV} was determined using the figure shown in Fig.2(a) of Eq. (1). One of three processes, including dynamic, static, or a mix of the two, can be used to control fluorescence quenching, but because each procedure is temperature-dependent, its underlying principles differ. It is projected that when temperatures rise, the quenching constants in the dynamic quenching process will also rise, leading to high diffusion coefficients. The quenching constant value for static quenching might, however, drop as a result of a loss in complex stability brought on by increasing temperatures. The quenching rate constant (kq) values demonstrate complex development was calculated according to the following equation:

$$k_q = \frac{K_{sv}}{\tau_0} \quad (2)$$

Thus, for a biomacromolecule, 10^{-8} s is the average lifetime of the fluorophore in the excited state, and kq is the bimolecular quenching rate constant [21, 22]. Stern-Volmer graphs for AA quenching of BSA fluorescence are revealed in Figure 4 at various temperature settings, while the K_{SV} and kq values are listed in Table 1.

Table 1. AA-BSA interaction characteristics at various temperatures

T(K)	Ksv ($Lmol^{-1}$)	Kq ($Lmol^{-1}$)	Kb ($Lmol^{-1}$)	n	ΔH^0 (kJ/mol^{-1})	ΔG^0 (kJ/mol^{-1})	ΔS^0 (kJ/mol^{-1})
303	5.47×10^5	5.47×10^{13}	6.4×10^6	1.18	-800.50	-1564.06	-2.52
308	1.53×10^5	1.53×10^{13}	2.54×10^4	0.67		-1576.16	
313	1.50×10^5	1.50×10^{13}	1.43×10^3	0.42		-1589.26	

According to this study, the quenching rate constant kq has a magnitude of 10^{13}. Moreover, the bimolecular quenching rate constant's value was revealed to be greater than 2×10^{10} L mol^{-1} s^{-1}, indicating a static quenching of the interaction between AA and BSA [22–24].

Binding sites and binding constant estimation

Both were calculated by applying what is known as the Modified Stern-Volmer equation:

$$\log\frac{F_0 - F}{F} = \log K_b + n\log[Q] \quad (3)$$

where K_b and n are the binding constant and number of binding sites, respectively [25, 26]. The intercept and slope of Fig. 2(b) correspondingly give the log K_b and n values. Table 1 displays the outcomes acquired under various temperature conditions. It was discovered that BSA and AA bind almost 1:1, and that the binding constant drops as temperature rises.

Calculation of the thermodynamic variables.

Hydrophobic, electrostatic, and van der Waals forces are the three primary forces involved in binding drugs and proteins. Enthalpy change (ΔH^0) and entropy change (ΔS^0), two thermodynamic quantities, define the forces that hold the process together. Subramanian and Ross looked at the connection between changes in binding forces and thermodynamic parameter values [27]. Hydrophobic forces predominate when $\Delta H^0>0$ and $\Delta S^0>0$, whereas van der Waals forces and hydrogen bonding predominate when $\Delta H^0<0$and $\Delta S^0<0$. When $\Delta H^0<0$ and$\Delta S^0>0$, electrostatic forces are regarded as the dominant forces. Van't Hoff equation can be utilised to calculate ΔH^0 and ΔS^0at the occurrence of small temperature differences [27, 28].

$$\ln K = -\frac{\Delta H^0}{RT} + \frac{\Delta S^0}{R} \quad (4)$$

where K_b is the binding constant at temperature T and R is the gas constant.

Plotting ln K against 1/ T results in a straight line. The resulting slope denotes the change in enthalpy (ΔH^0), whereas the intercept denotes the change in entropy (ΔS^0) (Fig. 2(c)). The free energy change (ΔG^0) can be calculated using the equation below:

$$\Delta G^0 = \Delta H^0 - T\Delta S^0 \quad (5)$$

Table 1 shows that the negative entropy change (ΔS^0) and the negative free energy change (ΔG^0) indicate that the AA-BSA complex spontaneously bound. The van der Waals forces and hydrogen bonding are the key driving force behind this process. The negative enthalpy change (ΔH^0) values indicates that the reaction is exothermic.

Synchronous fluorescence spectra of BSA

The benefits of the synchronous spectrofluorimetric technique are numerous and include spectral simplicity, sensitivity, spectral bandwidth, as well as restraining and avoiding different disturbing effects [29]. To explore the protein's microenvironment, it is extremely helpful to achieve the emission wavelength shift. By using synchronous fluorescence spectra at wavelength intervals ($\Delta\lambda$) of 60 nm and 15 nm, respectively, it is possible to identify the Trp and Tyr residues in BSA. It is also revealed in the synchronous BSA fluorescence spectra at $\Delta\lambda$=15nm and $\Delta\lambda$= 60 nm in Fig.3(a) and (b), respectively. In Fig. 3(b), at $\Delta\lambda$=60 nm, it was observed that the emission range maxima persisted unchanged, whereas at $\Delta\lambda$= 15 nm, a slight blue shift was seen as demonstrated in Fig. 3(a). Tyrosine residues were seen to have their surrounding polarity attenuated, indicating that this process took place in a hydrophobic environment. The observed spectrum change therefore suggests that BSA's conformation after interaction with AA [30].

Analysis of the displacement of the site marker

BSA is made up of three domains: I, II, and III, each of which is further broken down into two subdomains, A and B. The AA binding site in BSA was identified by a review of site marker measurements. Warfarin, Ibuprofen and haemin were chosen as competitive probes for sites I, II, and III, respectively [29–31]. The Stern-Volmer equation was used to calculate the binding parameters as a result of the three site markers' effects on the AA-BSA interaction (Fig. 4). The

binding of anisaldehyde and BSA was altered by the three competing reagents to varying degrees, as evidenced by the data in Table 2. It demonstrates that adding ibuprofen, warfarin and haemin significantly reduced the binding constant values of AA with BSA, indicating that these drugs may be able to displace the AA. In conclusion, these findings showed that AA binds to BSA at all three sites I, II and III. As seen from the table the better binding would be at the site I, as the binding constant was reduced to a greater extent, which is in good agreement with the findings of the molecular docking approach.

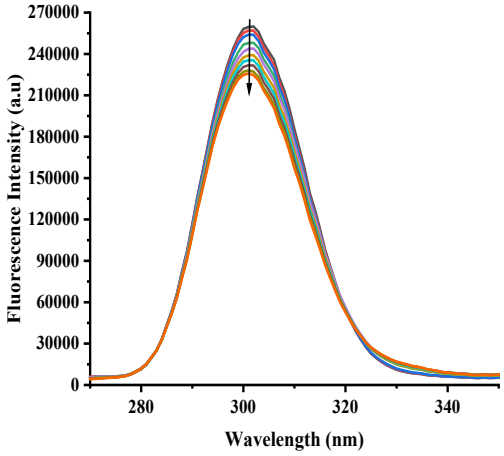

(a)

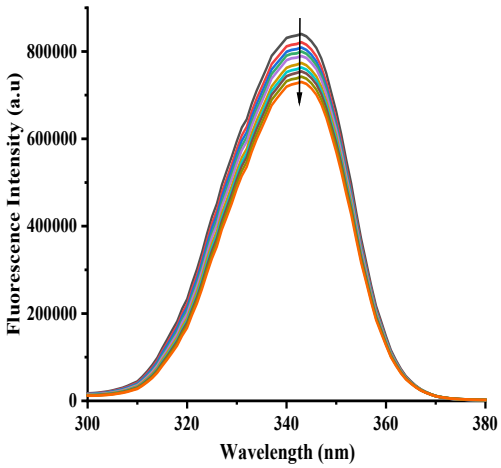

(b)

Figure 3. Synchronous fluorescence spectra of BSA (10 µM) at (a)Δλ 15 nm; (b) Δλ60 nm

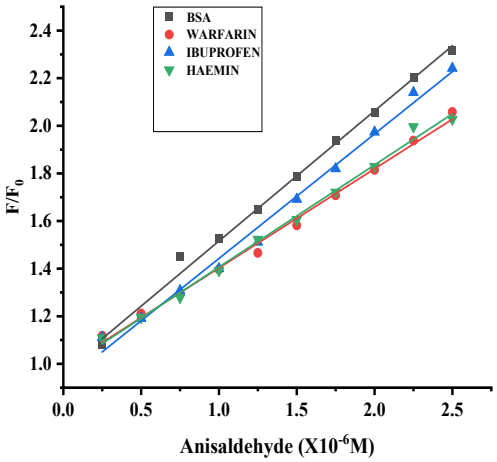

Figure 4. Pre- and post-marker addition Stern-Volmer plots for BSA quenching by AA.

Table 2. Stern-Volmer quenching constants for the AA-BSA interaction in the presence of site markers.

Site Marker	Ksv ($Lmol^{-1}$)	R^2	Standard Error
BSA+AA	5.47×10^5	0.99726	0.01434
BSA+AA+ WAR	4.17×10^5	0.99728	0.01089
BSA+AA+ IBU	5.23×10^5	0.99577	0.01707
BSA+AA+ HAEM	4.29×10^5	0.99738	0.01101

Circular dichroism studies

When globular proteins bind tiny ligands, circular dichroism is the preferred method for observing conformational changes and modifications in secondary structures. Using CD, the changes in BSA's confirmation after binding to anisaldehyde will be assessed in this section.The intermolecular forces necessary to maintain the secondary and tertiary structures are impacted by the binding of ligands to globular proteins; if these forces are harmed, the proteins' conformational states are altered. When a ligand binds to a protein, it alters the protein's structural conformation, and these changes in CD spectra are indicative of these structural changes [34]. The far UV CD spectra of free BSA and BSA-AA are displayed in Fig. 5. The image makes it clear that the CD spectra are just slightly changing. Natural BSA exhibits peaks at 209 nm and 220 nm, demonstrating that it is a protein with a high content of α-helices. In the presence of AA, there was a decrease in the secondary structure of BSA as evident from the decrease in two minima at 209 and 220 nm that are characteristic of α -helix.

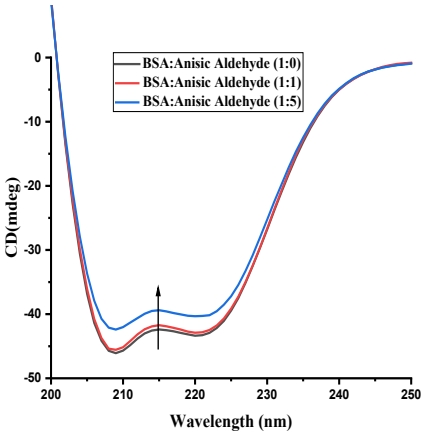

Figure 5. CD Spectra of BSA-AA

Molecular docking

Molecular docking is a practical simulation procedure for assessing the nature of drug-protein binding. It served as a means of validating the information discovered during the experimental study regarding the interactions and binding affinities of AA at its binding site in BSA. Findings from this method confirm earlier investigations of the site marker displacement, i.e., the binding of AA with BSA at site I of subdomain IIA (Fig.6 (a) and (b)). After binding with BSA, the configuration of AA was observed, giving a binding energy of -5.2kcal mol^{-1}. This AAligandis found in the active site residues Arg 256, Arg 217, Ile289, Ser 286 and Ala 290 (Fig. 6(c)). Also, the results of molecular docking suggested that hydrogen bonding and hydrophobic forces dominated the contact, which was in line with our thermodynamic analysis.

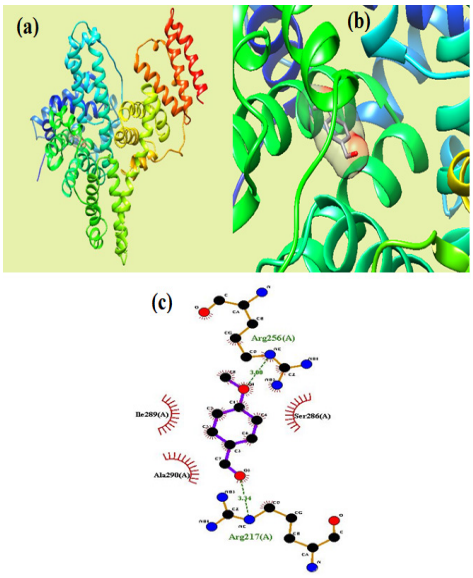

Figure 6 (a) AA docked in BSA; b) BSA and AA active site residues. The ribbon structure is used to illustrate the BSA. c) Hydrogen bonding and hydrophobic interactions in the AA interaction model at site I of BSA

CONCLUSION

With the aid of multi-spectroscopic and molecular docking techniques, the suggested work establishes the calculation of the AA-BSA binding under physiological circumstances. A variety of strategies have been used to perform extensive research. The binding of AA-BSA was discovered to be static quenching. Fluorescence spectroscopy data analysis was used to identify several binding factors. From the calculated n values it was depicted that AA and BSA bind in 1:1 ratio. The calculated thermodynamic parameter values for ΔH^0, ΔS^0 and ΔG^0 revealed that hydrophobic interactions and hydrogen bonding dominated other intermolecular forces in the interaction between AA and BSA.AA-BSA binding takes place at site I in subdomain IIA in accordance with the site marker technique that was confirmed by molecular docking experiments also. This study offers helpful information for a better comprehension of the pharmacokinetic behaviour of AA. The information in this study may contribute to a better understanding of the molecular processes underlying the negative side effects of AA, enhancing both its pharmacological and therapeutic efficacy. The findings supported the strong connection between AA and BSA as well as the simplicity of conveyance and removal, offering suggestions for additional research and study.

REFERENCES

1. P. Khan, S. Rahman, A. Queen, S. Manzoor, F. Naz, G. M. Hasan, S. Luqman, J. Kim, A. Islam, F. Ahmad, M. I. Hassan, *Sci Rep.,***7**, (2017).
2. G. I. Hernández-Bolio, J. A. Ruiz-Vargas, L. M. Peña-Rodríguez, *J. Nat. Prod.* (2019).
3. A. R. Guerra, M. F. Duarte, I. F. Duarte, *J. Agric. Food Chem.,* **66**, 10663 (2018).
4. H. N. Lv, S. Wang, K. W. Zeng, J. Li, X. Y. Guo, D. Ferreira, J. K. Zjawiony, P. F. Tu, Y. Jiang, *J. Nat. Prod*., **78**, 279 (2015).
5. G. R. Beecher, *Occurrence and Intake,* 1 (2003).
6. A. R. Guerra, M. F. Duarte, F. Duarte, *J. Agric . Food Chem*., **66**, 10663 (2018).
7. S. Zhao, C. H. Park, X. Li, Y. B. Kim, J. Yang, G. B. Sung, N. il Park, S. Kim, S. U. Park, *J. Agric. Food Chem.,* **63**, 8622 (2015).
8. S. Alban, G. Franz, R. Hänsel, W. Schier, O. Sticher, E. Spieß, E. Steinegger, *Pharmakognosie – Phytopharmazie,* Springer Berlin Heidelberg, 2013.
9. L. Yu, N. Guo, Y. Yang, X. Wu, R. Meng, J. Fan, F. Ge, X. Wang, J. Liu, X. Deng, *J. Ind. Microbiol. Biotechnol.*, **37**, 313 (2010).
10. S. Shreaz, R. Bhatia, N. Khan, S. Imran Ahmad, S. Muralidhar, S. F. Basir, N. Manzoor, L. A. Khan, *Microb. Pathog*., **51**, 277 (2011).
11. S. Khatun, Riyazuddeen, F. A. Qais, *J. Mol. Liq*., **299**, (2020).

12. Z. D. Zhivkova, V. N. Russeva, Analgesics · antiphlogistics antirheumatic drugs thermodynamic characterization of the binding process of sulindac to human serum albumin (2003).
13. N. Aggarwal, S Mehtab**,** S Maji, *Asian J. Chem.,* 29 (9), 2069 (2017).
14. S. M. S. Abdullah, S. Fatma, G. Rabbani, J. M. Ashraf, *J. Mol. Struct*.**, 1127**, 283 (2017).
15. J. A. Molina-Bolívar, F. Galisteo-González, C. Carnero Ruiz, M. Medina-Ó Donnell, A. Parra, *J. Lumin.,***156**, 141 (2014).
16. J. R. Lakowicz, Principles of Fluorescence Spectroscopy, 1 (2006).
17. G. Mocz, J. A. Ross, *Methods Mol. Biol.,***1008**, 169 (2013).
18. V. D. Suryawanshi, L. S. Walekar, A. H. Gore, P. V. Anbhule, G. B. Kolekar, *J. Pharm. Anal*.,**6**, 56 (2016).
19. B. L. Wang, D. Q. Pan, K. L. Zhou, Y. Y. Lou, J. H. Shi, *Spectrochim. Acta A Mol. Biomol Spectrosc*., **212**, 15 (2019).
20. S. Mehtab, H. Parmar, T.I. Siddiqi, A.S. Roy, Asian J. Res. Chem. **8** (2), 99 (2015).
21. Y. J. Hu, Y. Ou-Yang, C. M. Dai, Y. Liu, X. H. Xiao, *Mol. Biol. Rep.,* **37**, 3827 (2010).
22. E. Cobbina**,** S. Mehtab, I. Correia, G. Gonçalves, I. Tomaz, I. Cavaco, *J. Mexi. Chem. Soc.*, **57** (3), 180 (2013).
23. Y. J. Hu, Y. Liu, R. M. Zhao, J. X. Dong, S. S. Qu, *J. Photochem. Photobiol. A Chem.,***179**, 324 (2006).
24. F. Macii, T. Biver, *J. Inorg. Biochem.,***216**, (2021).
25. D. Yang, A. Singh, H. Wu, R. Kroe-Barrett, *Anal. Biochem.*, **508**, 78 (2016).
26. R. N. El Gammal, H. Elmansi, A. A. El-Emam, F. Belal, M. E. A. Hammouda, *Sci Rep***., 12**, (2022).
27. P. D. Ross, S. Subramanian, *Biochemistry,* **20**, 3096 (1981).
28. M. Otagiri, *Drug Metab. Pharmacokinet.,* **20**, 309 (2005).
29. A. S. Abdelhameed, A. M. Alanazi, A. H. Bakheit, H. W. Darwish, H. A. Ghabbour, I. A. Darwish, *Spectrochim. Acta A Mol. Biomol. Spectrosc.,***171**, 174 (2017).
30. S. K. Pawar, S. Jaldappagari, *J. Pharm. Anal.,*.**9**, 274 (2019).
31. G. Sudlow, D. Birkett, D. Wade, *Mol. Pharmacol.,* (1976).
32. X. X. Cheng, Y. Lui, B. Zhou, X. H. Xiao, Y. Liu, *Spectrochim. Acta A Mol. Biomol. Spectrosc.,***72**, 922 (2009).
33. Y. Z. Zhang, J. Dai, X. Xiang, W. W. Li, Y. Liu, *Mol. Biol. Rep.,* **37**, 1541 (2010).
34. A. Radha, A. Singh, L. Sharma, K. K. Thakur, in: Mater. Today Proc*.,* Elsevier Ltd, 2021.